DOI: 10.1002/chem.200601151

Electrocyclic Ring Opening of *cis*-Bicyclo[*m.n.*0]alkenes: The Anti-Woodward–Hoffmann Quest

Carlos Silva López, Olalla Nieto Faza, and Ángel R. de Lera*[a]

Abstract: The dubbed anti-Woodward–Hoffmann ring-opening reaction of *cis*-bicyclo[4.2.0]oct-7-ene to yield *cis,cis*-cycloocta-1,3-diene has been intensively studied with robust, high-level computational methods. This reaction has been found to proceed through a conrotatory allowed pathway to afford *cis,trans*-cycloocta-1,3-diene followed by *E* to *Z* isomerization, instead of a disrotatory forbidden pathway, as suggested. Computational calculations of kinetic isotope effects are consistent with this interpretation and the experimental values. The study of lower bicyclic homologues with [3.2.0], [2.2.0] and [2.1.0] skeletons indicates the feasibility of a mechanistic change towards the anti-Woodward–Hoffmann disrotatory path. This is clearly favored for the ring opening of the highly strained *cis*-bicyclo[2.1.0]pent-2-ene and is highly competitive with the conrotatory path for *cis*-bicyclo[2.2.0]hex-2-ene. Therefore, the rearrangement of the smallest bicyclic cyclobutene is predicted computationally to be an anti-Woodward–Hoffmann disrotatory electrocyclic ring-opening reaction.

Keywords: bicyclic compounds · electrocyclic reactions · ring-opening reactions · Woodward–Hoffmann rules

Introduction

Certainly one of the most important contributions to organic chemistry has been the seminal work by Woodward and Hoffmann regarding the feasibility of concerted reactions according to the conservation of orbital symmetry. Since their work was published starting with the famous communication in 1965,[1] the symmetry rules have been adopted as an essential toolbox for organic chemists. The success of Woodward and Hoffmann work is materialized in hundreds of textbooks and thousands of scientific articles citing their papers.[2] The fact that organic molecules seem to willingly comply with this set of rules readily prompted organic chemists to the quest for frontiers of the Woodward–Hoffmann rules. Despite numerous attempts, this experimental challenge has not been satisfied, partially due to the fact that seemingly anti-Woodward–Hoffmann reactions might actually proceed in a stepwise fashion where an allowed concerted reaction occurs yielding an intermediate which evolves to the apparent anti-Woodward–Hoffmann product,[3] or via diradicals.[4] Experimentally we can only refute this apparent subversion by isolating the intermediate but it is not possible to validate any proposed anti-Woodward–Hoffmann mechanism.

One of these mechanistic enigmas whose answer has been subject of debate for decades is the cycloisomerization of *cis*-bicyclo[4.2.0]oct-7-ene (**1a**) to *cis,cis*-cycloocta-1,3-diene (**5a**). Despite the large amount of accumulated data in the literature, the characterization of this transformation has challenged chemists until now. Very recently Baldwin and co-workers published a number of papers aimed to definitively address this issue.[5,6] After collecting data extracted from several kinetic studies, Baldwin and co-workers drew a tentative energy profile which combine the Arrhenius parameters for the overall reaction obtained by Branton and co-workers,[7] and are shown in Equation (1).

$$\log k = 14.13 - 43\,180/(2.303RT) \quad (1)$$

Arrhenius parameters for each of the steps involved in the putative, Woodward–Hoffmann allowed, conrotatory ring opening of **1a** were collected from previous experiments[8] or conveniently derived from kinetic and thermodynamic re-

[a] Dr. C. Silva López, Dr. O. Nieto Faza, Prof. Dr. Á. R. de Lera
Departamento de Química Orgánica
Facultad de Química
Universidade de Vigo
Lagoas Marcosende, 36310 Vigo, Galicia (Spain)
Fax: (+34) 986-811940
E-mail: qolera@uvigo.es

Supporting information for this article is available on the WWW under http://www.chemeurj.org/ or from the author.

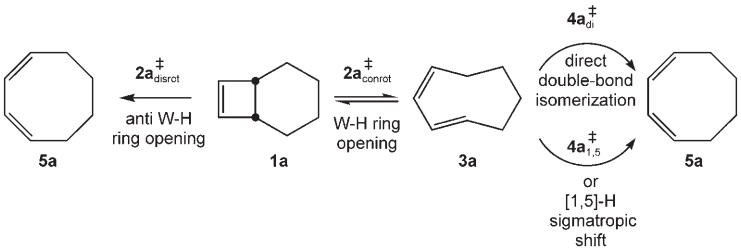

Scheme 1. Mechanistic alternatives for the ring-opening of *cis*-bicyclo[4.2.0]oct-7-ene (**1a**) as proposed by Baldwin and co-workers.[5,6]

lations (see Scheme 1).[9]

$$\log k_{\mathbf{3a}\rightleftharpoons\mathbf{1a}} = 13.14-27\,850/(2.303RT) \quad (2)$$

$$\log k_{\mathbf{1a}\rightleftharpoons\mathbf{3a}} = 13.3-33\,450/(2.303RT) \quad (3)$$

$$\log k_{\mathbf{3a}\rightleftharpoons\mathbf{5a}} = 14.0-37\,600/(2.303RT) \quad (4)$$

The equilibration of **1a**⇄**3a** is orders of magnitude faster than any of the candidate reaction steps yielding product **5a** (i.e., $k_{\mathbf{3a}\rightleftharpoons\mathbf{5a}}$ for the conrotatory alternative and $k_{\mathbf{1a}\rightleftharpoons\mathbf{5a}} = k$, if the reaction proceeds in only one step via disrotatory opening). Thus, the question of whether **5a** is formed from **1a** or **3a** cannot be answered easily through kinetic approaches.

The kinetic results leave open the question as to whether a symmetry allowed two-step mechanism or a forbidden one-step mechanism yielding *cis,cis*-1,3-cyclooctadiene **5a** from **1a** is taking place in the reaction pathway (see Scheme 1). Even the evolution of the possible intermediate obtained through the allowed conrotatory electrocyclic ring-opening step is still subject to debate since a sigmatropic shift and a $E\rightleftharpoons Z$ alkene isomerization are both compatible with the structure of the final product. Kinetic isotope effects and experiments with deuterium labeled molecules seem to discard the sigmatropic shift alternative[5,10] in an scenario in which the evolution of the intermediate is the rate-determining step. Despite these comprehensive experimental studies, a definitive answer to the mechanistic problem has not been provided yet.

Baldwin himself recognized in his work how difficult is the task of disclosing the nature of the mechanism through experimental studies and indicated how valuable a high level, preferentially multi-determinant, theoretical approach would be to shed light into this daunting problem.[6]

Prompted by the relevance of the challenge, we theoretically addressed the mechanistic issues of the **1a** to **5a** isomerization.[11] We showed by high-level computations that the ring opening of **1a** obeys the Woodward–Hoffmann rules, and proceeds stepwise through a conrotatory motion followed by a double-bond isomerization (Scheme 1, right). The mechanistic insights gleaned in this study led us to also consider the isomerization of the smaller bicyclo[*m.n.*0] homologues. We hereby provide a thorough study of electrocyclic ring-opening reactions of fused cyclobutenes aimed to not only clarify the above mechanism, but also establish under which conditions, if any, these molecules decline the Woodward–Hoffmann rules.

Computational Methods

Geometries and frequencies: The fact that some of the intermediates along the potential reaction mechanism exhibit a strong diradical character led us to consider performing a systematic methodology analysis coupled with the mechanistic study. Hartree–Fock is known to be very fragile with respect to spin-symmetry breaking, however, this is a convenient baseline to compare correlated methods. Dynamic correlation was introduced to the Hartree–Fock wavefunction via perturbational corrections using the Møller-Plesset implementation up to second order (MP2). The density functional theory[12] in its Kohn–Sham[13] formulation was also employed. A widely used hybrid functional (B3LYP) and its non-hybrid, GGA counterpart,[14–16] BLYP were included in the methodological study in order to account for the effect of Hartree–Fock exchange in hybrid functionals. Additionally, a modern meta-GGA functional (TPSS)[17] was also considered to test the performance of new functionals with explicit dependence on the kinetic energy density. Hybrid density functionals are known to mimic the effect of non-dynamic correlation, which was needed to correctly describe the diradical (or near degenerate) character, due to the self-interaction error introduced in local exchange functionals.[18]

Due to the high non-dynamic correlation present in the diradical intermediates a multireference approach was also taken into consideration. The near degeneracy problem was treated with MCSCF wavefunctions the active space of which include the π and σ electrons involved in the electrocyclic opening, thus a four electrons in four orbitals scheme was selected.

All the stationary points were optimized at the HF, MP2, DFT (B3LYP, BLYP and TPSS) and MCSCF levels of theory coupled with the widely employed 6-31G(d) basis set. Single reference methods (HF, MP2, DFT) were employed as implemented in Gaussian03[19] whereas all the multireference calculations were performed with the GAMESS package.[20] To ensure the validness of the computed data a stability check of the wavefunction[21] was performed for the one determinant methods (HF and DFT). Analytical frequencies were also computed for all the optimized geometries at the corresponding level of theory. Intrinsic Reaction Coordinate (IRC) calculations[22,23] were performed for all the ring-opening transition states optimized at the B3LYP/6-31G(d) level to ensure that the saddle points optimized actually connected reactants and products or intermediates in the potential energy surface.

Dynamic and non-dynamic correlation: It is well known that, on the one hand, solutions of the density functional theory and Møller-Plesset wavefunctions include an undetermined amount of dynamic correlation and, on the other hand, CASSCF wavefunctions can account mostly for an undetermined amount of non-dynamic correlation. A definitive approach should combine both at a reasonable computational cost. We have therefore included the treatment of dynamic correlation in the multireference scheme via perturbational theory, MRMP as implemented by Nakano.[24,25] Single point calculations at CASSCF(4,4)/6-31G(d) and B3LYP/6-31G(d) geometries were performed at the MRMP-(4,4)/6-31G(d). These sets of multilevel calculations are noted MRMP(4,4)/6-31G(d)//CASSCF(4,4)/6-31G(d) and MRMP(4,4)/6-31G(d)//B3LYP/6-31G(d), respectively. Thermal corrections to the free energy were obtained from unscaled frequency calculations at the theory level employed to obtain the geometry (i.e., CASSCF(4,4)/6-31G(d) and B3LYP/6-31G(d), respectively). Dynamic correlation is considered to be weakly dependent on the geometry whereas the non-dynamic portion of the electron correlation is supposed to be strongly dependent on the molecular geometry. We can therefore account for this effect since MRMP(4,4) energies were computed at two sets of geometries.[26]

The smaller *cis*-bicyclo[2.1.0]pent-2-ene (**1d**) is inadequately described with a 4,4-active space due to its high energy banana orbitals. These peculiar orbitals overlap very effectively with the π orbital of the cyclobutene moiety and are therefore involved in the ring-opening reactions. For this particular reaction a much bigger active space was considered. All the C–C bonding and antibonding orbitals were included in the active space resulting in CASSCF(14,14). This strategy ensures that any interaction of the molecular orbitals involved in the electrocyclic ring opening with the banana orbitals of the cyclopropane moiety will be included in the multiconfigurational description of the reaction.[27] The three stationary points along the ring-opening reaction of *cis*-bicyclo[2.1.0]pent-2-ene (**1d**) were optimized at the CASSCF(14,14)/6-31G(d) level. Perturbational corrections to the total energy were also computed resulting in MRMP-(14,14)/6-31G(d)//CASSCF(14,14)/6-31G(d) energies. Due to the high cost of these computations second derivatives of the energy (Hessian) could not be computed. As a consequence only density functional theory thermal corrections were available to obtain free energies. These corrections were therefore employed for multiconfigurational calculations at both CASSCF(14,14)/6-31G(d) and B3LYP/6-31G(d) geometries of **1d**, $\mathbf{2d}^{\pm}_{\text{disrot}}$ and **5d**.

Basis set size: We opted for a widely used, general purpose basis set due to the important differences in computational cost of the set of methods included in our work. Basis set size effects on both geometries and energies were considered notwithstanding. High-level DFT calculations were performed for the three alternate mechanisms of **1a** consisting of the following multilevel scheme.

- Geometry optimization at the B3LYP/6-31++G(d,p) and TPSS/6-31++G(d,p) levels.
- Stability check of the previous wavefunctions.
- Analytical frequencies at the B3LYP/6-31++G(d,p) and TPSS/6-31++G(d,p) levels.
- Energy refinement at the B3LYP/6-311++G(3df,2p) and TPSS/6-311++G(3df,2p) levels.

The differences in relative energies obtained with this multilevel methodology and with the ubiquitous 6-31G(d) basis were small (see Supporting Information).

We also took into consideration the effect of the basis set in the MRMP results by evaluating the MRMP energy at the B3LYP/6-31G(d) geometry with a bigger (triple ζ) basis set, noted as MRMP(4,4)/6-311+G(d,p)//B3LYP/6-31G(d). Very small energy differences were observed with these extended basis set calculations and thus, the more cost effective methodology described above was considered sufficiently accurate for every method included in this work. It should be taken into account, however, that correlation energy is always more efficiently recovered by perturbational methods with larger basis set.

Properties: In order to evaluate the aromatic character of several transition structures nucleus independent chemical shifts (NICS)[28] were computed using the gauge-independent atomic orbitals (GIAO).[29]

Kinetic isotope effects were computed at B3LYP/6-31G(d) and TPSS/6-31G(d) single reference levels with unscaled frequencies. Tunneling corrections were not taken into account in these computations.

Results

The relevant structures related to the electrocyclic ring opening of the entire series of fused cyclobutenes up to **1a** were computed with the aforementioned set of theoretical methods. These series include the isomerization of *cis*-bicyclo[4.2.0]oct-7-ene (**1a**), *cis*-bicyclo[3.2.0]hept-6-ene (**1b**), *cis*-bicyclo[2.2.0]hex-2-ene (**1c**) and *cis*-bicyclo-[2.1.0]pent-2-ene (**1d**) (see Scheme 2). The decrease in the number of ring atoms along the series considered here is aimed to find whether structural conditions exist where the ring strain and steric effects surmounts the symmetry rules

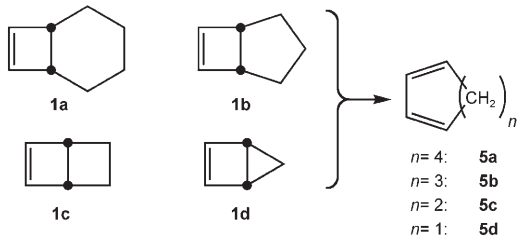

Scheme 2. Bicyclic structures included in this study represent a group of molecules with an increasing degree of ring strain.

and the anti-Woodward–Hoffmann disrotatory ring opening becomes the lowest lying transition state.

cis-Bicyclo[4.2.0]oct-7-ene isomerization

Single reference methods: Free energy profiles computed with single determinant methods for these three pathways are provided in the Supporting Information. It can be observed that Hartree–Fock cannot describe the reaction profile appropriately in those regions where the molecule exhibits some diradical character. This weakness is inherited to some extent by the MP2 approach. The latter correlation-corrected method is somehow more robust (i.e., we were able to optimize the geometry of $\mathbf{4a}^{\neq}_{di}$ which proved impossible in the Hartree–Fock scheme) but its energy results are unreliable due to the instability of the reference wavefunction.

DFT-based methods are known to be more robust with respect to spin-symmetry breaking.[21] The three functionals selected in this work confirmed this behavior. Geometry optimizations, stability check of the wavefunction and analytical Hessian calculations were successfully performed for all molecular geometries along the three alternative mechanisms. The stepwise mechanism via the [1,5]-hydrogen shift is very disfavored with respect to the stepwise mechanism via the direct rotation regardless of the functional employed (ca. 20 kcal mol^{-1}). This is in good agreement with recent experimental results from Baldwin[6] and previous experiments by Bramham and co-worker.[10] The concerted, disrotatory, ring opening seems to be noncompetitive as well. The fact that the [1,5]-sigmatropic shift is less favored than a symmetry forbidden electrocyclic opening captivated our attention. Geometrical analysis of the *cis*,*trans*-cycloocta-1,3-diene intermediate **3a** and the [1,5]-sigmatropic hydrogen shift transition state $\mathbf{4a}^{\neq}_{1,5}$ suggests that the suprafacial requirement for the sigmatropic rearrangement involves a considerable amount of strain to be added to an already distorted intermediate and shifts the energy of this transition state above that of the disrotatory alternative.

We observed that despite their superior behavior, electron density functionals do not agree perfectly either with the experimental evidence or among themselves regarding relative activation barriers.[11]

Multireference methods: Inspection of the reaction profiles obtained with multireference methods (see Supporting Information) suggest that unless both dynamic and nondynamic correlation are taken into account the description of the reaction mechanism is rather poor. The fact that CASSCF underestimated the direct isomerization barrier was not a surprise since it is well known that this methodology tends to overstabilize diradical configurations. It is also accepted that the introduction of dynamic correlation corrections helps to balance this bias and improves dramatically the quality of the computed activation energies.[30] Inclusion of electron correlation via perturbative methods in the CASSCF wavefunction results in a lowering of the conrotatory ring-opening activation barrier whereas both, the disrotatory ring-opening transition state, $\mathbf{2a}^{\neq}_{disrot}$, and the direct isomerization transition state, $\mathbf{4a}^{\neq}_{di}$, raise their energy with respect to the reactant **1a** (4–5 and 2–3 kcal mol^{-1}, respectively, depending on the level of theory used to obtain their geometries). This results in the correct description of the overall energy profile, the conrotatory ring-opening step is a fast step in the mechanism whereas the $E \rightarrow Z$ isomerization is the energy bottleneck. MRMP(4,4) accounts for free energies of activation and reaction fairly well taking into account the disparity of correlation effects governing the different mechanistic steps present along the profile and the fact that we decided to employ a modest basis set for the sake of efficiency (37.7 and -6.9 kcal mol^{-1} at the MRMP(4,4)/6-31G(d)//CASSCF(4,4)/6-31G(d) level versus 43.2 and -8.7 kcal mol^{-1} experimentally measured).

Kinetic isotope effects: Due to the impossibility of characterizing the mechanistic alternative operating in the cycloisomerization of **1a** by means of the rate constants, Baldwin and co-workers devised a number of KIE experiments (see Scheme 3) aimed to discard some of the alternatives considered in Scheme 1 and to determine which of these mechanisms is actually taking place in the reaction flask.

The experiment **I** illustrated in Scheme 3 was designed to detect whether the [1,5]-sigmatropic shift was a feasible mechanistic pathway. The quadruple deuterium substitution at positions C2 and C5 would involve a large primary isotope effect if the reaction proceeds through a [1,5]-sigmatropic shift even at high temperatures.[31] The measured $k_H/k_D([D_4])$ ratio of 1.17 clearly ruled out the possibility of a hydrogen shift taking place at the rate-limiting step of the reaction path. In previous work it was also noted that this $k_H/k_D([D_4])$ ratio could be interpreted as an effective $k_H/$

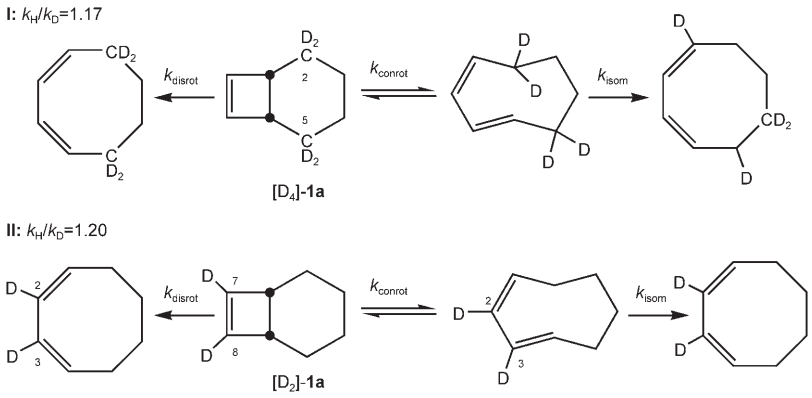

Scheme 3. Kinetic isotope effect experiments performed by Baldwin and co-workers.[5,6]

$k_D = 1.04$ per deuterium, but we consider that this approximation could only apply if the reaction proceeds through the disrotatory ring opening, for which the four labels are roughly equivalent. But it is clearly inappropriate to analyze the [1,5]-H shift since only one deuterium label is involved in the primary KIE whereas the other three labels would contribute to the kinetic isotope effect in a lower extent (they would promote β and γ secondary isotope effects, probably in opposite directions due to the gain of coordination at one terminus of the pericyclic reaction and the loss of coordination at the other). A related experiment based on isotopic substitutions in *cis*,*trans*-cycloocta-1,3-diene was performed by Bramham and Samuel and also discarded the [1,5]-H shift.[10] All of these experimental results are in good agreement with our predictions based on the high energy of the [1,5]-H sigmatropic shift transition state $\mathbf{4a}^{\ddagger}_{1,5}$.

Experiment **II** was devised to discard the involvement of the double-bond isomerization via internal rotation and thus support the disrotatory, anti-Woodward–Hoffmann mechanism, as the only viable alternative. The 7,8-[D_2]-*cis*-bicyclo-[4.2.0]oct-7-ene reactant [D_2]-**1a** converts to deuterated monocyclic dienes at positions C2 and C3 after the cycloisomerization (see Scheme 3). In previous work[6] it was assumed that a considerable KIE would be expected, due to the deuterium label on the *trans*-double bond, if the rate-limiting step involves a *cis*,*trans*→*cis*,*cis* isomerization through internal rotation. In fact, several experimental KIE values for *cis*→*trans* isomerizations of substrates with deuterium labels on the isomerizing alkene groups have been reported with k_H/k_D values of around 2.0 at room temperature.[32] It was also assumed that a disrotatory opening would produce a small KIE, reflecting the mild changes in the hybridization and geometry occurring at the internal positions of the cyclobutene moiety during the concerted pathway. The experimental KIE measured for [D_2]-**1a**, $k_H/k_D([D_2]) = 1.20$, was considered too low with respect to the expected value. Again, it was surmised that this effect could be partitioned in $k_H/k_D = 1.10$ per deuterium. This approximation is, however, only valid for the disrotatory mechanism, in which both deuterated positions are chemically equivalent, not for the $E \rightarrow Z$ double-bond isomerization rate-limiting step. We therefore decided to compute these isotope effects to account for the contribution of each of the chemically different deuterium labels in the internal rotation step.

Scheme 4 shows five pairs of KIE computed at two different levels of theory. The first set, **A**, reproduces the experiment performed by Baldwin on the 7,8-dideuterated derivative of **1a**. Reactions **B** and **C** are aimed to account for the contributions of the chemically non-equivalent deuterium substitutions in **A**. Reactions **D** and **E** were included to check an alternative isotopic substitution which would be more compatible with the experiments suggesting values $k_H/k_D \approx 2.0$ for *cis*→*trans* isomerizations (i.e., deuterium substitution at both ends of the double bond). The computed KIE for reaction **A** is indeed very small ($k_H/k_D([D_2] = 1.08)$ compared with the expected values reported by Baldwin. The contribution of each deuterium label is, however, very different and cannot be straightforwardly approximated to 1.04. We have computed the contribution of each independent deuterium label and we found that the deuterium located on the *trans*-double bond shows a k_H/k_D ratio of 1.27, thus higher than the double isotopic substitution (see reaction **B** in Scheme 4) and closer to the expected values. Accordingly, the isotope effect contribution due to single substitution at the *cis*-double bond of **3a** shows an inverse KIE (reaction **C**) which cancels out most of the KIE created by the substitution on the *trans*-double bond. Thus, it can be concluded that the KIE due to substitution on the *trans*-double bond is actually compatible with other related experiments[10] but was masked by the deuterium label on the *cis*-double bond. We also considered further alternative isotopic substitutions which are more similar to the aforementioned experiments reported by Bramham and Samuel.[10] In reaction **D** both ends of the isomerizing double bond are deuterium substituted and the computed k_H/k_D is 2.2, which is in excellent agreement with previously discussed values. Due to the particular bond pattern in this molecule and the hindrance introduced by the bicyclic structure, the deuterium labeled C_{sp^2} in reaction **E** suffers nearly all the motion associated with the reaction coordinate in the *trans*→*cis* isomerization step whereas its internal C_{sp^2} counterpart remains still. This feature makes the substitution at the bridging position exhibit a higher KIE than the internal isotopomer (see reaction **B** and **E** in Scheme 4).

An alternative deuterium labeling pattern which might help to determine what reaction mechanism is followed in the opening of **1a** has been proposed recently in the basis of KIE computations.[11]

Isomerization of *cis*-bicyclo[*m.n.*0]alkenes: In order to explore the strain conditions for competitive Woodward–Hoffmann and anti-Woodward–Hoffmann reaction mechanisms we considered systematic ring contractions in the parent bicyclic system **1a**. We therefore studied the conrotatory and disrotatory alternatives for thermal rearrangement of **1b–d**.

Single reference methods: Due to the poor performance Hartree–Fock based methods showed for the parent system we consider here only the DFT approaches (results from Hartree–Fock and MP2 are available in the Supporting Information). Free energy profiles for the [4.2.0]-, [3.2.0]-, [2.2.0]- and [2.1.0]-bicyclic homologues are provided in Table 1. These profiles suggest that the largest systems (**1a** and **1b**) undergo ring opening through a favored conrotatory pathway whereas the high energy disrotatory alternatives imply high order saddle points ($\mathbf{2a}^{\ddagger}_{disrot}$ and $\mathbf{2b}^{\ddagger}_{disrot}$ with three and two imaginary normal modes, respectively). The energy difference between the two mechanistic alternatives (ca. 15 and 10 kcal mol^{-1} for **1a** and **1b**) is sufficient to ensure total discrimination at ordinary temperatures. This considerable energy gap renders the competition quite unfeasible even in the case of DFT methods providing some error due to higher spin mixing in the diradical species. We nevertheless

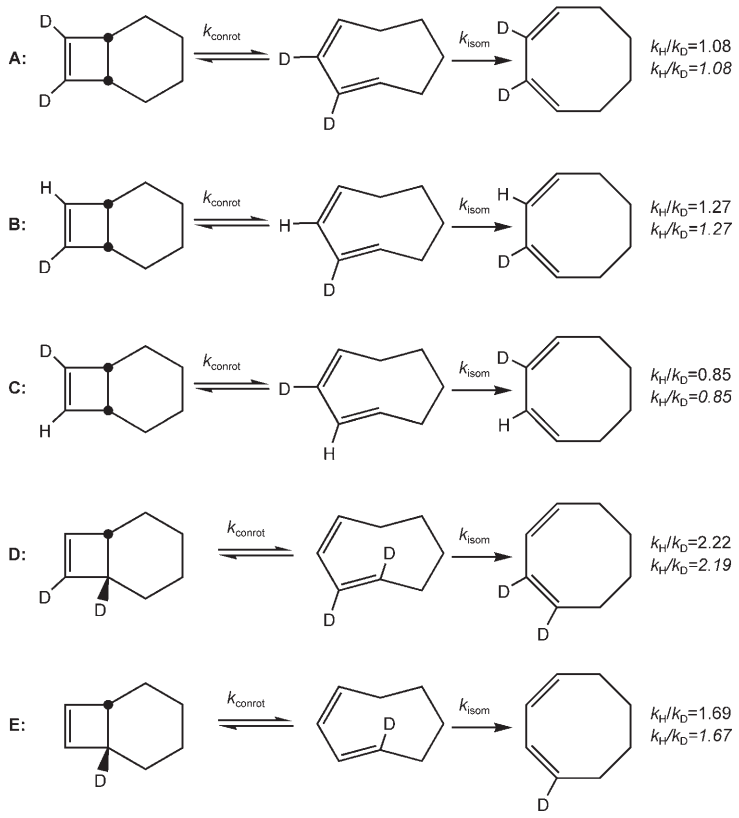

Scheme 4. Kinetic isotope effects computed at B3LYP/6-31G(d) (plain) and TPSS/6-31G(d) (italics) levels for the *cis*,*trans*→*cis*,*cis* isomerization through internal rotation of **3a**.

computed these profiles at a multireference level to ensure the quality of the computed activation energies and, at the same time, compare the performance of these functionals (see below).

Inspection of the reaction profiles summarized in Table 1 suggest that, similar to **3a**, the *cis*,*trans* reaction intermediate could be detected for thermal opening of **1b**. Smaller molecules present contrasting features. The bicyclo-[2.2.0]hex-2-ene **1c** shows a kinetically irrelevant activation barrier associated with the *cis*, *trans*→*cis*,*cis* isomerization (less than 1 kcal mol^{-1} for *cis*, *trans*-cyclohexa-1,3-diene **3c**). Interestingly, a forbidden disrotary transition state was located as the only pathway for the thermal ring opening of **1d**. The four-electron ring-opening activation barrier seems to be nearly ring size independent and varies within 30–36 kcal mol^{-1} whereas the alternative disrotatory ring opening is highly dependent on the ring size. The activation energy to reach $\mathbf{2}^{\neq}_{disrot}$ steadily decreases from 49–52 kcal mol^{-1} for systems **1a** to 22–24 kcal mol^{-1} for **1d**. It can be observed that the energy drop is roughly 10 kcal mol^{-1} per -CH_2- substracted in the bicyclic structure. These results clearly indicate a crossing point in the preferred mechanism at **1c**.

In order to provide further information regarding the electronic features of the conrotatory and disrotatory transition structures, the NICS were computed along an axis perpendicular to the opening cyclobutene ring 3 Å above and below the center of the cycle. Since some of the transition structures exhibit considerable diradical character, it is interesting to compare them with the corresponding closed shell solution of the Hamiltonian. This comparison can be interpreted as an indication of how

Table 1. DFT disrotatory and conrotatory ring opening free energy profiles (298.15 K, 1 atm) of **1a–d**.

	[4.2.0]			[3.2.0]			[2.2.0]			[2.1.0]		
	BLYP	B3LYP	TPSS	BLYP	B3LYP	TPSS	BLYP	B3LYP	TPSS	BLYP	B3LYP	TPSS
disrotatory opening[a]												
1	0.00	0.00	0.00	0.00	0.00	0.00	0.00	0.00	0.00	0.00	0.00	0.00
$\mathbf{2}^{\neq}_{disrot}$	49.43	51.08	51.83	42.90	44.48	45.17	31.55	33.70	33.97	22.03	23.04	23.89
5	−8.93	−6.68	−3.26	−20.14	−17.99	−14.15	−37.60	−37.25	−31.82	−47.56	−47.78	−42.43
N. Imag.[a]		3			2			1			1	
conrotatory opening[b]												
1	0.00	0.00	0.00	0.00	0.00	0.00	0.00	0.00	0.00	0.00	0.00	0.00
$\mathbf{2}^{\neq}_{conrot}$	30.36	35.25	33.36	29.50	34.38	32.60	29.25	34.03	32.95	–	–	–
3	3.00	5.80	7.49	16.84	20.37	21.55	18.90	23.10	24.18	–	–	–
$\mathbf{4}^{\neq}_{di}$	33.68	34.68	36.28	33.13	33.89	35.47	21.71	23.22	24.96	–	–	–
5	−8.93	−6.68	−3.26	−20.14	−17.99	−14.15	−37.60	−37.25	−31.82	−47.56	−47.78	−42.43
exptl.[c] E_{rxn}		−8.7			−10.8			−36.0			−47.8	
exptl. $E^{\neq}$		43.2			45.5			33.0			26.9	

[a] Certain disrotatory opening transition structures were computed imposing a C_s symmetry to their geometry. Some of these structures are not true transition states but saddle points of higher order. The number of negative eigenvalues for each Hessian is provided to distinguish transition structures from higher order saddle points. [b] Several stationary points associated with the conrotatory ring opening could not be located and are indicated with a dash. [c] For experimental results see ref. [6] and references therein.

strong the anti aromatic character in a transition structure must be to force the electrons into a diradical state (i.e., to lose some dynamic correlation), and thus, it can help measure the causes of the instability of the closed-shell configuration. NICS values were therefore computed for all the conrotatory and disrotatory transition structures. The restricted wavefunction was also employed to compute the NICS for the latter, and the corresponding data is provided in Figure 1.

These computations show mild aromatic character in conrotatory transition structures $\mathbf{2a}^{\neq}_{conrot}$, $\mathbf{2b}^{\neq}_{conrot}$ and $\mathbf{2c}^{\neq}_{conrot}$ whereas all the disrotatory alternatives display values suggesting antiaromaticity (see Figure 1). The closed-shell configurations of disrotatory transition states show strong antiaromatic character ($NICS_{min}$ values ranging from −20 to −30 ppm). Disrotatory transition states are partially (some of them strongly) diradical in nature, its wavefunction presents moderate to strong spin contamination and spin-symmetry break can help reduce the high energy associated with an anti-aromatic structure. To estimate the energy relieved by the molecule adopting a singlet diradical configuration we performed single-point calculations of the open shell and the closed shell wavefunctions at the transition state geometries. The energy difference between the closed and the open shell configurations is 15.2, 11.0, 6.4 and 5.5 kcal mol^{-1} for $\mathbf{2a}^{\neq}_{disrot}$, $\mathbf{2b}^{\neq}_{disrot}$, $\mathbf{2c}^{\neq}_{disrot}$ and $\mathbf{2d}^{\neq}_{disrot}$, respectively, which very well justifies the spin-symmetry breaking. Figure 1 indicates that the reduction of the anti-aromatic character is also considerable for the diradical configuration (NICS values ranging between −20 to −30 ppm in closed shell wavefunctions decrease to −2 to −10 ppm in the diradical configuration).

Multireference methods: A summary of the results obtained from multireference methods is provided in Table 2. Computations were performed on CASSCF and B3LYP geometries for the conrotatory and the disrotatory ring opening of **1a–d**. In general, differences due to the level of theory chosen for the optimized geometry are small with the remarkable exception of the ring opening profiles for **1c**. The conrotatory ring-opening transition structure $\mathbf{2c}^{\neq}_{conrot}$ could not be located at the CASSCF/6-31G(d) level due to the overestimation of non-dynamic correlation in this method. The highly competitive transition state found if B3LYP/6-31G(d) geometries are used is a strong indication of the importance of the dynamic correlation. It also suggests that this transition structure might have also been located if geometry optimizations at the MRMP level were possible.

The same strain and ring-size trends observed with density functionals are also found with multireference methods. Interestingly, the double bond *cis*,*trans*→*cis*,*cis* isomerization process is a paradigmatic diagnostic to evaluate the feasibility of the conrotatory, stepwise mechanism. The isomerization free energy is, roughly, −10, −35, and −55 kcal mol^{-1} for the [4.2.0], [3.2.0], and [2.2.0] systems, respectively, at the MRMP level. This energy trend correlates well with the *trans* C-C-C-C double bond dihedral angle at intermediates **3**: 132, 107 and 79°, respectively. Both, the energetic and the geometric parameters very well account for the fact that a conrotation leading to a hypothetic, and extremely strained, *cis*,*trans*-cyclopenta-1,3-diene is not feasible.

Further inspection of values in Table 2 reveals the effect of the Hartree–Fock exchange in B3LYP. Interestingly, B3LYP activation energies of the conrotatory ring opening are systematically higher than those provided by pure functionals (5 and 2 kcal mol^{-1} approximately compared with

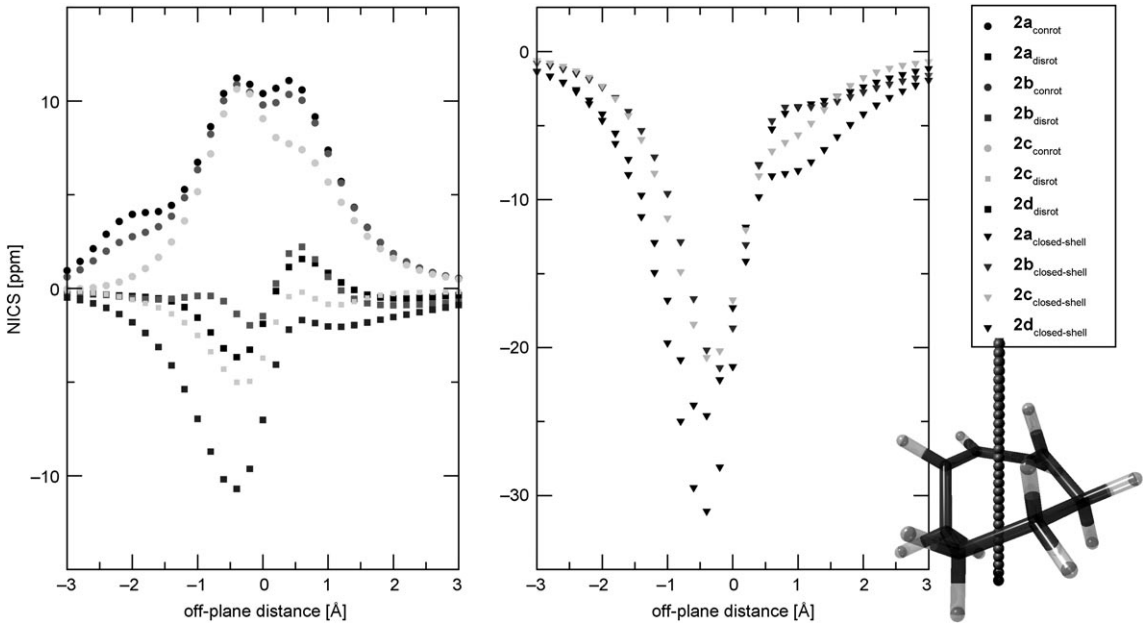

Figure 1. Nucleus independent chemical shifts computed along a perpendicular axis located at the center of mass of the four-membered ring at conrotatory and disrotatory ring opening transition structures of **1a–d**. The axis obtained for the conrotatory ring opening of **1a** is depicted.

Table 2. CASSCF and MRMP disrotatory and conrotatory ring opening free energy profiles (298.15 K, 1 atm) for the isomerization of **1a**–**d**.

	[4.2.0]		[3.2.0]		[2.2.0]		[2.1.0][a]	
	CASSCF	MRMP	CASSCF	MRMP	CASSCF	MRMP	CASSCF	MRMP
free energy values computed at CASSCF geometries								
disrotatory opening[b]								
1	0.00	0.00	0.00	0.00	0.00	0.00	0.00	0.00
$\mathbf{2}^{\neq}_{\text{disrot}}$	46.52	52.18	38.84	43.50	26.25	30.30	21.96	21.80
5	−11.67	−6.88	−23.26	−17.65	−45.26	−40.21	−49.60	−45.13
N. Imag.[b,c]	2		2		1		1	
conrotatory opening[d]								
1	0.00	0.00	0.00	0.00	0.00	0.00	0.00	0.00
$\mathbf{2}^{\neq}_{\text{conrot}}$	39.04	30.83	37.48	30.08	–	–	–	–
3	1.10	3.58	15.04	17.24	15.68	16.66	–	–
$\mathbf{4}^{\neq}_{\text{di}}$	34.76	37.66	33.10	35.72	18.53	20.33	–	–
5	−11.67	−6.88	−23.26	−17.65	−45.26	−40.21	−54.76	−49.92
free energy values computed at B3LYP geometries								
disrotatory opening[c]								
1	0.00	0.00	0.00	0.00	0.00	0.00	0.00	0.00
$\mathbf{2}^{\neq}_{\text{disrot}}$	46.55	50.67	38.44	41.19	24.80	27.69	19.52	19.19
5	−11.08	−6.29	−22.94	−17.34	−45.00	−39.79	−49.34	−45.11
N. Imag.[b,c]	3		2		1		1	
conrotatory opening[d]								
1	0.00	0.00	0.00	0.00	0.00	0.00	0.00	0.00
$\mathbf{2}^{\neq}_{\text{conrot}}$	40.33	31.20	39.57	29.96	36.86	28.47	–	–
3	1.68	3.63	15.68	17.36	16.90	16.85	–	–
$\mathbf{4}^{\neq}_{\text{di}}$	35.15	37.28	33.30	35.02	17.68	17.45	–	–
5	−11.08	−6.29	−22.94	−17.34	−45.00	−39.79	−54.98	−50.12
exptl.[e] E_{rxn})	−8.7		−10.8		−36.0		−47.8	
exptl. $E^{\neq}$	43.2		45.5		33.0		26.9	

[a] The ring opening of **1d** was computed with an expanded active space since the inclusion of the cyclopropane ring moiety banana orbitals in the active space was required (see section on Computational Methods). [b] Certain disrotatory opening transition structures were computed imposing a C_s symmetry to their geometry. Some of these structures are not true transition states but saddle points of higher order. The number of negative eigenvalues for each Hessian is provided to distinguish transition structures from higher order saddle points. [c] B3LYP and CASSCF frequency calculations differ in the number of negative eigenvalues of the hessian for $\mathbf{2}^{\neq}_{\text{conrot}}$ (see text). [d] Several stationary points associated with the conrotatory ring opening could not be located and are indicated with a dash. [e] For experimental results see ref. [6] and references therein.

BLYP and TPSS, respectively, see Table 1). This trend is also found in Table 2 when comparing CASSCF against MRMP free energies. CASSCF relative free energies for the conrotatory ring opening are 8–10 kcal mol^{-1} higher compared with MRMP. Actually MRMP free energies closely resemble the values provided by BLYP and/or TPSS.

Regarding the disrotatory, anti-Woodward–Hoffmann, ring opening, the three functionals employed provide very similar results which are in close agreement with MRMP free energies. A marginal discrepancy in the number of imaginary frequencies at these transition structures can also be observed. This is due to the fact that CASSCF couples the internal rotation between positions C3 and C4 with the conrotatory normal mode in $\mathbf{2a}^{\neq}_{\text{disrot}}$. It is well known that common density functionals mimic the effects of non-dynamic correlation because of the self-interaction error inherent to the local and GGA exchange functionals.[18] This smaller contribution of the self-interaction error improves hybrid functionals with respect to their LDA/GGA counterparts when dealing with transition-state energies. Conversely, it also implies that hybrid functionals provide a poorer description of molecules with large multireference character. The overall result seems to be the wrong order in the relative free energies of activation computed with B3LYP (see free energies for $\mathbf{2a}^{\neq}_{\text{conrot}}$ and $\mathbf{4a}^{\neq}_{\text{di}}$ in Table 1).

Conclusions

Several theoretical methods have been applied to study the cycloisomerization of **1a** and smaller ring size homologues through the conrotatory ring opening (followed by [1,5]-H shift or thermal $E \rightarrow Z$ isomerization) or the potential anti-Woodward–Hoffmann disrotatory ring opening. Black-box, single reference methods based on density functional theory provide qualitatively correct results but are inadequate and inconclusive to decide which of the alternative mechanistic pathways is the lowest energy one. This problem arises from the inconsistent and unbalanced description of the dynamic and non-dynamic correlation in density functionals. MRMP seems to be a robust and balanced method to account for both kinds of electron correlation and it provides activation barriers consistent with the experimental evidence.

Our computations predict that the most favorable mechanistic alternative for the thermal rearrangement of **1a** and **1b** to the corresponding *cis*,*cis*-cycloalkadienes **5a** and **5b** involves a conrotatory ring opening (thus, a symmetry allowed mechanism) followed by a higher energy direct $E \rightarrow Z$ isomerization. This pathway is compatible with the kinetic results published elsewhere (for **1a**) in terms of activation energies and rate-limiting steps. Kinetic isotope effects have been used to prove and/or refute the participation of the

disrotatory ring opening, the $E \rightarrow Z$ isomerization via a [1,5]-H shift and the $E \rightarrow Z$ isomerization via internal rotation. Our computations are in good agreement with the KIE reported in previous work and also helped in the location of errors in one KIE experiment design (or in the interpretation derived from its results) which led to think the rearrangement of **1a** proceeds through an anti-Woodward–Hoffmann electrocyclic ring opening.

A disrotatory (anti-Woodward–Hoffmann) electrocyclic opening is highly competitive with the conrotatory ring opening $E \rightarrow Z$ isomerization mechanism in the rearrangement of *cis*-bicyclo[2.2.0]hex-2-ene (**1c**). Furthermore, the highly strained *cis*-bicyclo[2.1.0]pent-2-ene (**1d**) is predicted to undergo thermal opening only through the disrotatory pathway to *cis*,*cis*-cyclopenta-1,3-diene (**5d**).

Acknowledgement

The authors are grateful to the Ministerio de Educacin y Ciencia (FPU scholarships and SAF2004-07131 grant), the European Community (EPITRON-Contract No. 518417) and the Centro de Supercomputacin de Galicia (CESGA) for allocation of computation time.

[1] R. B. Woodward, R. Hoffmann, *J. Am. Chem. Soc.* **1965**, *87*, 395–397.
[2] S. Wilkinson, *Chem. Eng. News* **2003**, *81*, 59.
[3] O. N. Faza, C. S. López, R. Álvarez, A R. de Lera, *Org. Lett.* **2004**, *6*, 901–904.
[4] E. R. Davidson, J. J. Gajewski, C. A. Shook, T. Cohen, *J. Am. Chem. Soc.* **1995**, *117*, 8495–8501.
[5] J. E. Baldwin, S. S. Gallagher, P. A. Leber, A. Raghavan, *Org. Lett.* **2004**, *6*, 1457–1460.
[6] J. E. Baldwin, S. S. Gallagher, P. A. Leber, A. S. Raghavan, R. Shukla, *J. Org. Chem.* **2004**, *69*, 7212–7219.
[7] G. R. Branton, H. M. Frey, R. F. Skinner, *Trans. Faraday Soc.* **1966**, *62*, 1546–1552.
[8] J. J. Bloomfield, J. McConaghy, S. John, A. G. Hortmann, *Tetrahedron Lett.* **1969**, *10*, 3723–3726.
[9] A. T. Cocks, H. M. Frey, *J. Chem. Soc. B* **1970**, 952–954.
[10] J. Bramham, C. J. Samuel, *J. Chem. Soc. Chem. Commun.* **1989**, 29–30.
[11] C. S. López, O. N. Faza, A. R. de Lera, *Org. Lett.* **2006**, *8*, 2055–2058.
[12] P. Hohenberg, W. Kohn, *Phys. Rev.* **1964**, *136*, B864–B871.
[13] W. Kohn, L. Sham, *Phys. Rev. A* **1965**, *140*, A1133–A1138.
[14] A. D. Becke, *Phys. Rev. A* **1988**, *38*, 3098–3100.
[15] A. D. Becke, *J. Chem. Phys.* **1993**, *98*, 5648–5652.
[16] C. Lee, W. Yang, R. G. Parr, *Phys. Rev. B* **1988**, *37*, 785–789.
[17] J. Tao, J. P. Perdew, V. N. Staroverov, G. E. Scuseria, *Phys. Rev. Lett.* **2003**, *91*, 146401.
[18] D. Cremer, *Mol. Phys.* **2001**, *99*, 1899–1940.
[19] Gaussian 03, Revision C.02, M. J. Frisch, G. W. Trucks, H. B. Schlegel, G. E. Scuseria, M. A. Robb, J. R. Cheeseman, J. A. Montgomery, Jr., T. Vreven, K. N. Kudin, J. C. Burant, J. M. Millam, S. S. Iyengar, J. Tomasi, V. Barone, B. Mennucci, M. Cossi, G. Scalmani, N. Rega, G. A. Petersson, H. Nakatsuji, M. Hada, M. Ehara, K. Toyota, R. Fukuda, J. Hasegawa, M. Ishida, T. Nakajima, Y. Honda, O. Kitao, H. Nakai, M. Klene, X. Li, J. E. Knox, H. P. Hratchian, J. B. Cross, V. Bakken, C. Adamo, J. Jaramillo, R. Gomperts, R. E. Stratmann, O. Yazyev, A. J. Austin, R. Cammi, C. Pomelli, J. W. Ochterski, P. Y. Ayala, K. Morokuma, G. A. Voth, P. Salvador, J. J. Dannenberg, V. G. Zakrzewski, S. Dapprich, A. D. Daniels, M. C. Strain, O. Farkas, D. K. Malick, A. D. Rabuck, K. Raghavachari, J. B. Foresman, J. V. Ortiz, Q. Cui, A. G. Baboul, S. Clifford, J. Cioslowski, B. B. Stefanov, G. Liu, A. Liashenko, P. Piskorz, I. Komaromi, R. L. Martin, D. J. Fox, T. Keith, M. A. Al-Laham, C. Y. Peng, A. Nanayakkara, M. Challacombe, P. M. W. Gill, B. Johnson, W. Chen, M. W. Wong, C. Gonzalez, J. A. Pople, Gaussian, Inc., Wallingford, CT, **2004**.
[20] M. W. Schmidt, K. K. Baldridge, J. A. Boatz, S. T. Elbert, M. S. Gordon, J. H. Jensen, S. Koseki, N. Matsunaga, K. A. Nguyen, S. Su, T. L. Windus, M. Dupuis, J. A. Montgomery, Jr., *J. Comput. Chem.* **1993**, *14*, 1347–1363.
[21] R. Bauernschmitt, R. Ahlrichs, *J. Chem. Phys.* **1996**, *104*, 9047–9052.
[22] C. Gonzalez, H. B. Schlegel, *J. Chem. Phys.* **1989**, *90*, 2154–2161.
[23] C. Gonzalez, H. B. Schlegel, *J. Phys. Chem.* **1990**, *94*, 5523–5527.
[24] H. Nakano, *J. Chem. Phys.* **1993**, *99*, 7983–7992.
[25] H. Nakano, *Chem. Phys. Lett.* **1993**, *207*, 372–378.
[26] B. Ramachandran, *J. Phys. Chem. A* **2006**, *110*, 396–403.
[27] Notice that this wide active space will also allow a much more efficient recovery of dynamic correlation since more CI-like configurations are included.
[28] P. v. R. Schleyer, C. Maerker, A. Dransfeld, H. Jiao, N. J. R. v. Hommes, *J. Am. Chem. Soc.* **1996**, *118*, 6317–6318.
[29] K. Wolinski, J. F. Hinton, P. Pulay, *J. Am. Chem. Soc.* **1990**, *112*, 8251–8260.
[30] V. Guner, K. S. Khuong, A. G. Leach, P. S. Lee, M. D. Bartberger, K. N. Houk, *J. Phys. Chem. A* **2003**, *107*, 11445–11459.
[31] [1,5]-H sigmatropic shifts in cycloocta-1,3,6-triene and *cis*-penta-1,3-diene present k_H/k_D values of 5.0 at 120 °C and 5.1 at 200 °C, respectively (see ref. [6]).
[32] See ref. [6], and references therein.

Received: August 9, 2006
Revised: December 17, 2006
Published online: March 20, 2007

